



Article

Effects of NaOH Activation on Adsorptive Removal of Herbicides by Biochars Prepared from Ground Coffee Residues

Yong-Gu Lee ¹, Jaegwan Shin ² , Jinwoo Kwak ², Sangwon Kim ², Changgil Son ², Kyung Hwa Cho ³ and Kangmin Chon ^{1,2,*} 

¹ Department of Environmental Engineering, College of Engineering, Kangwon National University, 1 Kangwondaehak-gil, Chuncheon-si, Gangwon-do 24341, Korea; yglee19@kangwon.ac.kr

² Department of Integrated Energy and Infra system, Kangwon National University, 1 Kangwondaehak-gil, Chuncheon-si, Gangwon-do 24341, Korea; jgshin13@kangwon.ac.kr (J.S.); kh01kpw@kangwon.ac.kr (J.K.); swkim9521@kangwon.ac.kr (S.K.); numer5@kangwon.ac.kr (C.S.)

³ School of Urban and Environmental Engineering, Ulsan National Institute of Science and Technology (UNIST), 50 UNIST-gil, Eonyang-eup, Ulju-gun, Ulsan 689-798, Korea; khcho@unist.ac.kr

* Correspondence: kmchon@kangwon.ac.kr; Tel.: +82-33-250-6352

Abstract: In this study, the adsorption of herbicides using ground coffee residue biochars without (GCRB) and with NaOH activation (GCRB-N) was compared to provide deeper insights into their adsorption behaviors and mechanisms. The physicochemical characteristics of GCRB and GCRB-N were analyzed using Brunauer–Emmett–Teller surface area, Fourier transform infrared spectroscopy, scanning electron microscopy, and X-ray diffraction and the effects of pH, temperature, ionic strength, and humic acids on the adsorption of herbicides were identified. Moreover, the adsorption kinetics and isotherms were studied. The specific surface area and total pore volume of GCRB-N (405.33 m²/g and 0.293 cm³/g) were greater than those of GCRB (3.83 m²/g and 0.014 cm³/g). The GCRB-N could more effectively remove the herbicides ($Q_{e,exp}$ of Alachlor = 122.71 μmol/g, $Q_{e,exp}$ of Diuron = 166.42 μmol/g, and $Q_{e,exp}$ of Simazine = 99.16 μmol/g) than GCRB ($Q_{e,exp}$ of Alachlor = 11.74 μmol/g, $Q_{e,exp}$ of Diuron = 9.95 μmol/g, and $Q_{e,exp}$ of Simazine = 6.53 μmol/g). These results suggested that chemical activation with NaOH might be a promising option to make the GCRB more practical and effective for removing herbicides in the aqueous solutions.

Keywords: NaOH activation; biochars; competitive adsorption; ground coffee residue; herbicides



Citation: Lee, Y.-G.; Shin, J.; Kwak, J.; Kim, S.; Son, C.; Cho, K.H.; Chon, K. Effects of NaOH Activation on Adsorptive Removal of Herbicides by Biochars Prepared from Ground Coffee Residues. *Energies* **2021**, *14*, 1297. <https://doi.org/10.3390/en14051297>

Academic Editor: Wei-Hsin Chen

Received: 15 January 2021

Accepted: 22 February 2021

Published: 26 February 2021

Publisher's Note: MDPI stays neutral with regard to jurisdictional claims in published maps and institutional affiliations.



Copyright: © 2021 by the authors. Licensee MDPI, Basel, Switzerland. This article is an open access article distributed under the terms and conditions of the Creative Commons Attribution (CC BY) license (<https://creativecommons.org/licenses/by/4.0/>).

1. Introduction

The increasing use of herbicides with different action modes (e.g., photosynthesis inhibition, plant growth regulation) to enhance agricultural production can lead to non-point source pollutants of surface water and groundwater through herbicides leaching and runoff from agricultural fields [1–3]. Even at very low concentrations (<1 μg/L), the biochemical properties (i.e., bioaccumulation and persistence) of herbicides have posed potential risks to the aquatic ecosystem and human health due to toxicity and carcinogenicity [4]. Several studies of alachlor (ALA), the chloroacetamide class of herbicides, one of the most used preemergence herbicides globally, were conducted due to its serious health effects (e.g., carcinogenicity and reproductivity) for humans than other herbicides [5,6]. Moreover, the previous studies reported that diuron (DIU) effectively governed algal blooms associated with cyanobacteria by inhibiting photosynthesis [3,7]. However, the persistence of DIU in the water posed the prevention of oxygen production in the aquatic ecosystem could severely deplete dissolved oxygen, causing the suffocation of aquatic organisms [8]. Although simazine (SIM), chlorotriazine herbicide, has been extensively used since the 1950s for selective weed control, it can generate mutagenicity, reproductive and immune toxicities on the fish and amphibians due to low biodegradation rate and high ecological

toxicity [9–11]. Therefore, based on these reasons, wastewater treatment techniques have achieved significant importance as increasing attention to global environmental concerns for herbicide pollution of the water sources.

Conventional wastewater treatment processes, including precipitation, coagulation-flocculation, sedimentation, and sand filtration, are insufficient to eliminate the herbicides from the direct and indirect discharge of the herbicide contaminated wastewater [12]. Although membrane processes and advanced oxidation processes can effectively remove the herbicides from aqueous solutions, these techniques are not applicable in all wastewater treatment plants since they high energy consumption and operating costs and production of hazardous oxidation by-products [4,13]. Meanwhile, the adsorption process is recognized as the most efficient option for removing herbicides from the wastewater and cheap operating cost [14]. Activated carbon (AC), one of the adsorbent materials, has been become widely used for wastewater treatment due to its porous surface area, controllable pore structure, thermo-stability, and low acid/base reactivity [15]. Although AC has a high-affinity to hydrophobic compounds, the DIU and SIM in the presence of NH groups are more hydrophilic herbicides than other herbicides, and their removal efficiencies can be reduced by the AC [13].

Biochar is carbon-rich materials (e.g., charcoal) produced by pyrolysis of biomass wastes (e.g., agricultural and food residues) under limited oxygen conditions [16]. Furthermore, it may be an excellent alternative adsorbent material to activated carbon due to the physicochemical properties of biochar (i.e., high surface areas, large total pore volumes, and unique functional groups) [17]. The production of effective biochar can be influenced by carbonization and activation conditions (e.g., types of biomass, temperature, retention time, and activating agents) [18]. The chemical activation method using activating treatments (i.e., alkali, acid, and oxidative agents) can increase the number of oxygen-containing functional groups on the surface of biochar, enhancing the possibility of specific binding (e.g., hydrogen bonding and π - π electron donor-acceptor interactions) [19]. In particular, alkali-treated biochars compared with oxidative and acid-treated biochars have presented improved specific surface areas and total pore volumes, which are sufficient to remove pollutants in the aqueous solutions [20]. Over 600 million tons of ground coffee residues are disposed into the environment annually worldwide after the extraction process for coffee powder and instant coffee [21]. Ground coffee residues are known to contain a high concentration of carbohydrates (e.g., mannose, glucose, and galactose) and OH and C=O functional groups [22]. Therefore, the ground coffee residues biochar (GCRB) may be regarded as a potential resource to produce eco-friendly and low-cost adsorbents to remove herbicides. Nevertheless, a comprehensive study on the effects of the GCRB physicochemical characteristics and applying chemical activation treatment for GCRB on removing herbicides in aqueous solutions has not been performed yet.

The primary purpose of this study was to provide valuable insights into the effects of the sodium hydroxide (NaOH) activation on the properties in the GCRB related to the adsorption mechanisms of ALA, DIU, and SIM. Hence, the differences in GCRB and NaOH-activated GCRB (GCRB-N) (i.e., bulk elements and functional groups) were identified and compared the kinetic and isotherm models of three different herbicides. Furthermore, the effects of solution pH and temperature, and the presence of ionic strength and humic acids in the solutions on the adsorptions of the ALA, DIU, and SIM by GCRB and GCRB-N were examined.

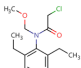
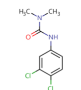
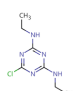
2. Materials and Methods

2.1. Chemicals and Herbicides

All chemicals were of analytical grade and available commercially. ALA (2-chloro-*N*-(2,6-diethylphenyl)-*N*-(methoxymethyl)acetamide), DIU (1-(3,4-dichlorophenyl)-3,3-dimethylurea), and SIM (6-chloro-*N*₂,*N*₄-diethyl-1,3,5-triazine-2,4-diamine), sodium chloride (NaCl), NaOH, and hydrochloric acid (HCl), phosphoric acid (H₃PO₄), and humic acids were purchased from Sigma Aldrich (St. Louis, MO, USA). Deionized (DI) water

(resistivity > 18.2 M Ω cm⁻¹, Barnstead Nanopure Water System, Lake Balboa, CA, USA) was utilized to make stock solutions of the ALA, DIU, and SIM (concentration of each herbicide = 1 mmol/L). These stocks were stored at 4 °C in the dark prior to use. The acetonitrile (C₂H₃N) and methanol (CH₃OH) were obtained from Thermo-Fisher Scientific (HPLC grade, Waltham, MA USA). The physicochemical properties of ALA, DIU, and SIM are presented in Table 1.

Table 1. Physicochemical Characteristics of the Herbicides.

Compounds (Abbreviation)	Formula	Structure	MW (g/mol)	Health Hazards ^a	Charge ^b			Log D ^a			pK _a ^a	Solubility ^c in Water (g/L, pH 7)
					pH 3.0	pH 7.0	pH 11.0	pH 3.0	pH 7.0	pH 11.0		
Alachlor (ALA)	C ₁₄ H ₂₀ ClNO ₂		269.77	Inhalation, Irritation (Skin)	0	0	0	3.59	3.59	3.59	-	0.240
Diuron (DIU)	C ₉ H ₁₀ Cl ₂ N ₂ O		233.09	Inhalation, Irritation (Eyes, Skin)	0	0	0	2.53	2.53	2.53	13.18	0.042
Simazine (SIM)	C ₇ H ₁₂ ClN ₅		201.66	Irritation, Organs damage (Liver, Kidney)	1	0	0	0.60	1.78	1.78	4.23	0.006

^a CAMEO Chemicals (<https://cameochemicals.noaa.gov>, accessed on 5 February 2021). ^b ChemAxon (<http://www.chemicalize.org>, accessed on 2 January 2021). ^c Hazardous Substances Data Bank (<http://pubchem.ncbi.nih.gov>, accessed on 2 January 2021).

2.2. Preparation of GCRB and GCRB-N

The detailed preparation procedures of the GCRB for the NaOH activation were the same as those in our previous study [23]. As briefly explained, the preparation procedures of the GCRB for the NaOH activation as follows: ground coffee residues were collected from a local coffee shop in Chuncheon-si (Gangwon Province, Korea), followed by rinsing with DI water and overnight drying in the oven at 105 °C. The NaOH activation is mixed with 15 g of the dried ground coffee residues and 4 M NaOH solution (200 mL) under moderate stirring at room temperature (20 ± 0.5 °C) for 2 h and then dried at 105 °C in the oven for 12 h. Both the GCRB and GCRB-N were pyrolyzed using a tubular furnace (PyroTech, Namyangju-si, Korea) at 800 °C for 2 h with a linear rise of 10 °C/min under N₂ atmosphere (the flow rate = 0.25 L/min). After cooled down to room temperature, the produced GCRB and GCRB-N were rinsed with DI water several times and dried at 105 °C in the oven for 12 h. The dried GCRB and GCRB-N were passed through a 100 mesh sieve to keep their uniform sizes and then stored in a desiccator before usage.

2.3. Batch Adsorption Experiments

The adsorption isotherms of the herbicides were examined with five different initial concentrations (the concentration of each herbicide = 10, 20, 30, 40, and 50 µmol/L) under the controlled conditions (working volume = 20 mL, adsorbents dosage = 50 mg/L, agitation speed = 150 rpm, contact time = 24 h, temperature = 25 °C, and pH = 7.0). The competitive adsorption kinetics (the concentration of each herbicide = 10 µmol/L) was investigated by varying the contact time (0, 0.5, 1, 2, 4, 8, 12, 16, and 24 h). The effects of pH and ionic strength on the competitive adsorptions of the herbicides (the concentration of each herbicide = 10 µmol/L) were evaluated by adjusting solution pHs (pH = 3.0, 7.0, and 11.0) and ionic strengths (ionic strength = 0.0, 0.025, 0.050, 0.075, and 0.100 M) using HCl and NaOH, and NaCl, respectively. The interferences of humic acids with the adsorptions of the herbicides (the concentration of each herbicide = 10 µmol/L) by the GCRB and GCRB-N were identified by adding 5 mg/L of humic acids. All adsorption experiments were performed in triplicates using a shaking incubator (Vision Scientific, Daejeon-si, Korea). After batch adsorption experiments, the samples were filtered using glass fiber filters

(GF/F, nominal pore size = 0.7 μm , Whatman, Clifton, NJ, USA) and stored in a refrigerator at 4 $^{\circ}\text{C}$ before analyses. The diagram of batch adsorption experiments is shown in Figure 1.

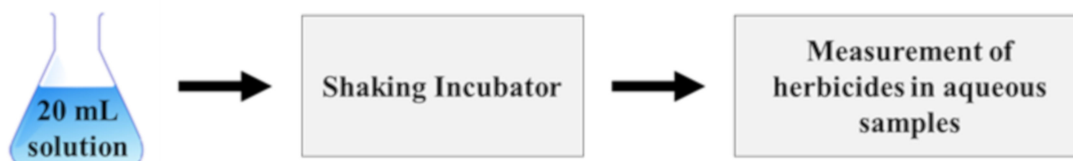


Figure 1. The diagram for batch experiments for adsorption of herbicides in aqueous solution.

2.4. Analytical Methods

The specific surface area, the average pore size, and the total pore volume of the GCRB and GCRB-N were evaluated by nitrogen gas (N_2) adsorption/desorption isotherms at 77.3 K (ASAP 2020 plus, Micromeritics, GA, USA). The specific surface areas of the GCRB and GCRB-N were measured using the Brunauer–Emmett–Teller (BET) model, and the average pore size and total pore volume were calculated by the Barrett–Joyner–Halenda (BJH) method (the adsorbed quantity of N_2 at $P/P_0 = 0.995$) [24]. The elemental compositions of the GCRB and GCRB-N were determined using a EuroEA3000 CHNS-O Analyzer (EuroVector S.p.A, Via Tortona, Milan, Italy). The ash contents were analyzed by deducting the carbon (C), hydrogen (H), oxygen (O), and nitrogen (N) contents from the total amount of the GCRB and GCRB-N. The atomic ratios of $[(\text{O} + \text{N})/\text{C}]$ and H/C represented the polarity and the aromaticity of the GCRB and GCRB-N, respectively [25]. Fourier transform infrared (FTIR) spectroscopy (FT-IR Frontier Optica, Perkin Elmer, Waltham, MA, USA) with KBr pellet (biochar:KBr = 1:50, w/w) was used to investigate the functional groups of the GCRB and GCRB-N in the wavenumber range of 400 and 4000 cm^{-1} . The surface morphologies of GCRB and GCRB-N were observed using a scanning electron microscope (SEM; S-4800, Hitachi, Tokyo, Japan) equipped with energy dispersive X-ray (EDX) spectroscopy. The crystal structure of GCRB and GCRB-N was identified using X-ray diffraction (XRD, D/Max-2500, Rigaku, Tokyo, Japan). The concentrations of the three different herbicides in the aqueous solution were quantified using high-performance liquid chromatography (HPLC) fitted with an ultraviolet absorbance (UVA) detector (SPD-10AVP, Shimadzu, Kyoto, Japan) and a XDB C18 column (ZORBAX Eclipse[®], 4.6 mm \times 150 mm, inner diameter = 5 μm , Agilent, Santa Clara, CA, USA) at a constant flow rate of 1.0 mL/min for 15 min. Acetonitrile/0.05 M phosphoric acid (50:50, v/v) at a flow rate of 1.0 mL/min were worked as the mobile phase for ALA, DIU, and SIM. The wavelength of the UVA detector was set at 210 nm for the ALA, DIU, and SIM.

The amounts of the adsorbed herbicides on the GCRB and GCRB-N at equilibrium (Q_e , $\mu\text{mol/g}$) were calculated by the following Equation (1):

$$Q_e = \frac{(C_0 - C_e)V}{M} \quad (1)$$

where C_0 ($\mu\text{mol/L}$) and C_e ($\mu\text{mol/L}$) are the initial concentration and equilibrium concentration of ALA, DIU, and SIM, respectively, V (L) is the volume of the aqueous solution, and M (g) is the amount of adsorbents.

The removal rate of the herbicides by the GCRB and GCRB-N was calculated by the following Equation (2):

$$\text{Removal efficiency}(\%) = \frac{C_0 - C_e}{C_0} \times 100. \quad (2)$$

The isotherms data were analyzed with the Langmuir and Freundlich models, and the adsorption kinetics were examined with the pseudo first and second order models [26]. The selected two isotherms and kinetic models could adequately explain the adsorption

behaviors of herbicides (ALA, DIU, and SIM) on the GCRB and GCRB-N. The Langmuir model was defined as described by Equation (3):

$$Q_e = Q_{max} \frac{K_L C_e}{1 + K_L C_e} \quad (3)$$

where C_e ($\mu\text{mol/L}$) is the concentration of each herbicide at equilibrium, Q_{max} ($\mu\text{mol/g}$) and K_L ($\text{L}/\mu\text{mol}$) associated with the maximum adsorption capacity and the adsorption energy, respectively.

The Freundlich model was presented as written by Equation (4):

$$Q_e = K_F C_e^{1/n} \quad (4)$$

where K_F ($\mu\text{mol}^{1-(1/n)} \text{L}^{1/n}/\text{g}$) and n are constants correspond to the relative maximum adsorption capacity and the dimensionless adsorption intensity, respectively.

The pseudo first order might be represented as follows by Equation (5):

$$Q_t = Q_e \left(1 - \frac{1}{\exp(k_1 t)}\right) \quad (5)$$

where Q_t , ($\mu\text{mol/g}$) is the amounts of the adsorbed herbicides on the GCRB and GCRB-N at the predetermined time t , t (h) is the adsorption time (0, 0.5, 1, 2, 4, 8, 12, 16, 24 h), and k_1 (1/h) is the rate constant of pseudo first order.

The pseudo second order model might be written as the following Equation (6):

$$Q_t = Q_e \left(1 - \frac{1}{1 + Q_e k_2 t}\right) \quad (6)$$

where k_2 ($\text{g}/\mu\text{mol}\cdot\text{h}$) is the rate constant of pseudo second order.

3. Results and Discussions

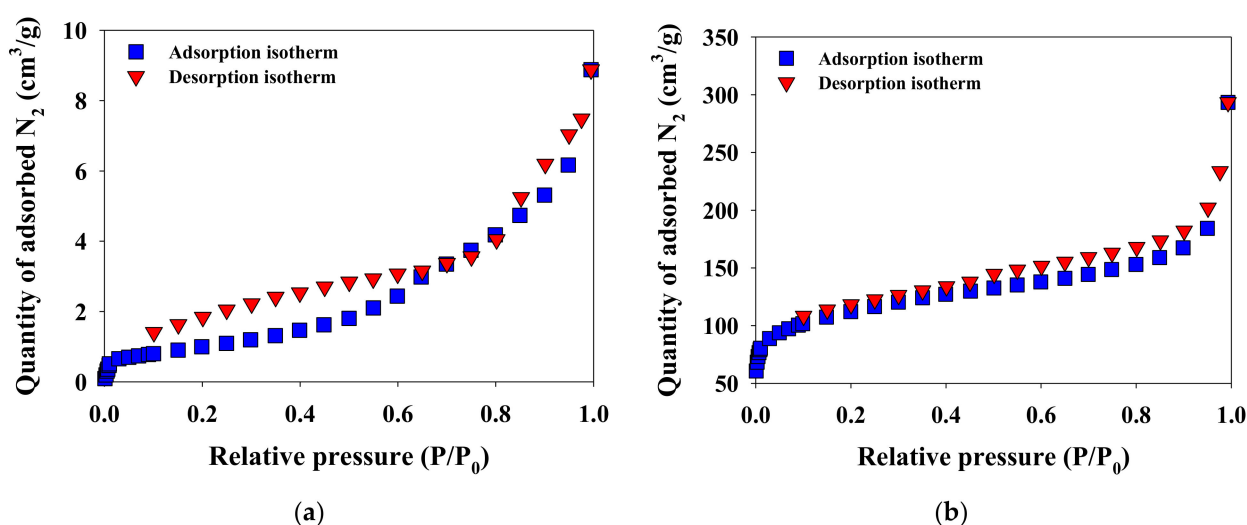
3.1. Characteristics of the GCRB and GCRB-N

3.1.1. Bulk Elemental Composition and Functional Groups Analyses

The bulk element constitutions (i.e., C, H, O, and N), ash contents, atomic ratios, specific surface area, average pore size, total pore volume, and BET isotherms (i.e., N_2 adsorption/desorption isotherms) for the GCRB and GCRB-N related to the adsorption capacity are summarized in Table 2 and Figure 2. The bulk element contents of the GCRB (C = 83.5%, H = 1.8%, O = 3.7%, and N = 3.4%) were relatively greater than those of the GCRB-N (C = 82.9%, H = 1.4%, O = 3.6%, and N = 1.3%) since some organic matter was removed in the NaOH activation procedures [27]. The atomic ratios of H/C, O/C, and (O+N)/C are commonly identified for aromaticity, surface hydrophobicity, and polarity, respectively [28]. These results demonstrated that the aromaticity (H/C = 0.022 of the GCRB and H/C = 0.017 of the GCRB-N) and polarity ((O+N)/C = 0.085 of the GCRB and (O+N)/C = 0.060 of the GCRB-N) of the GCRB were found to increase due to NaOH activation. However, the hydrophobicity of the GCRB-N (O/C = 0.043) was not significantly different compared with that of the GCRB (O/C = 0.044). The specific surface area and the pore volume of the GCRB-N (specific surface area = $405.33 \text{ m}^2 \text{ g}^{-1}$ and pore volume = $0.293 \text{ cm}^3 \text{ g}^{-1}$) were considerably increased (specific surface area: >105 times higher; pore volume: >21 times higher) compared with that of the GCRB (specific surface area = $3.83 \text{ m}^2 \text{ g}^{-1}$ and pore volume = $0.014 \text{ cm}^3 \text{ g}^{-1}$) due to the pore distribution change by NaOH [29]. However, the averaged pore size of the GCRB-N (3.05 nm) was significantly smaller than that of the GCRB (5.59 nm). These findings could explain the enhanced porous structures of GCRB-N associated with their adsorption capacities [23]. Thus, the GCRB-N are expected to improve the removal of herbicides from aqueous solutions compared with the GCRB.

Table 2. The physicochemical properties of the GCRB and GCRB-N.

	Properties	GCRB	GCRB-N
Bulk elemental constitutions (%)	C	83.5	82.9
	H	1.8	1.4
	O	3.7	3.6
	N	3.4	1.3
	Ash	7.6	10.8
Atomic ratio	H/C	0.022	0.017
	O/C	0.044	0.043
	(O+N)/C	0.085	0.060
Specific surface area (m ² g ⁻¹)	3.83	405.33	
Average pore size (nm)	5.59	3.05	
Total pore volume (cm ³ g ⁻¹)	0.014	0.293	

**Figure 2.** The N₂ adsorption/desorption isotherms of the (a) GCRB and (b) GCRB-N (at 77.3 K in the relative pressure range of 0.01–0.99).

The FT-IR spectra of the GCRB and GCRB-N are shown in Figure 3. The IR peaks of the GCRB at 3448 cm⁻¹, 1616 cm⁻¹, and 1134 cm⁻¹ are attributed to the OH stretching of alcohols, C=O stretching of carboxylic acids, and C-O-C stretching of ethers, respectively [30,31]. The GCRB-N present IR peaks at 3440–3160 cm⁻¹ and 1650–1450 cm⁻¹, corresponding to the OH stretching of alcohols and C=O stretching of carboxylic acids, respectively. The high intensities of IR peaks (i.e., OH stretching of alcohols and C=O stretching of carboxylic acids) for the GCRB may explain that the characteristic of relatively hydrophilic surfaces of the GCRB compared with that of GCRB-N.

3.1.2. SEM-EDX and XRD Analyses

The SEM images and the XRD spectra of the GCRB and GCRB-N are shown in Figure 4. Smooth and flat shape structures were found for the GCRB, but the GCRB-N had irregular and porous structures (Figure 4a,b). These observations clearly show that the NaOH activation might change the surface morphological characteristics of the GCRB associated with the herbicide adsorptions [32]. The SEM-EDX results of the GCRB and GCRB-N might be provided evidence that the influence of NaOH activation on the differences in the components of GCRB and GCRB-N. The GCRB-N composed of C (82.72%), O (16.15%), Na (0.80%), and Pt (0.33%), while the GCRB consisted of C (92.87%), O (6.92%), Na (0.04%), and Pt (0.17%). The atomic percentage of Na in the GCRB-N is 20 times greater than that of GCRB. A possible explanation for these findings is that there is a high possibility of Na incorporation on the GCRB surface during NaOH activation. Pt contents on the

GCRB and GCRB-N surfaces are caused by the sputter-coating with Pt for the preventing charging effects [33]. The XRD spectra of GCRB and GCRB-N solely present the peaks of amorphous carbons ($2\theta = 23^\circ$ and 43°) (Figure 4c,d). These results are demonstrated that XRD might not be sensitive to the crystalline structure changes caused by NaOH activation, and it could be less effective in identifying the surface properties difference in the GCRB and GCRB-N.

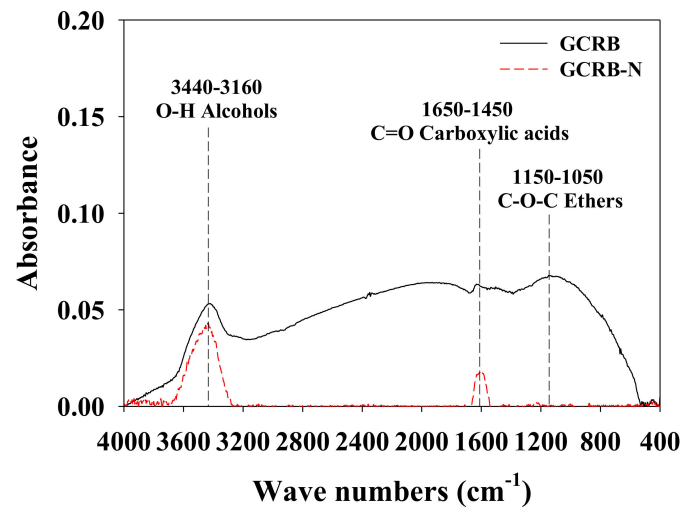


Figure 3. The FT-IR spectra of the GCRB and GCRB-N.

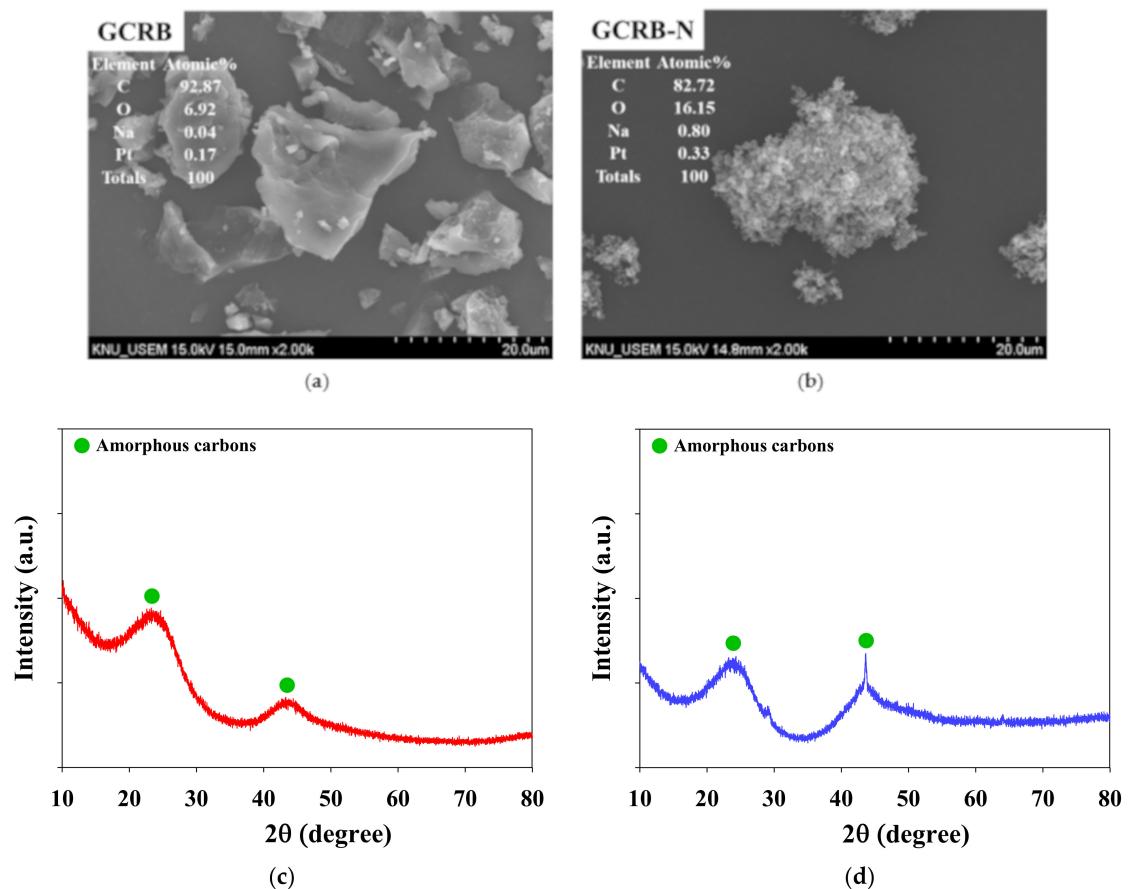


Figure 4. The SEM images of the (a) GCRB and (b) GCRB-N (magnification = 2000), and the XRD spectra of the (c) GCRB and (d) GCRB-N.

3.2. Adsorption of Herbicides: Kinetics Studies

The adsorption kinetics of the herbicides by the GCRB and GCRB-N were examined by shaking the mixed solutions for the 24 h (Figure 5). The adsorption process could be divided two-phase for herbicides using GCRB and GCRB-N: (i) phase I, contact period ≤ 4 h and (ii) phase II, contact period >4 h. Phase I is the removal rates of the herbicides quickly enlarged as the physical adsorption occurred onto the surfaces of the GCRB and GCRB-N. Phase II is the removal rates of the herbicides slowly improved by the GCRB and GCRB-N since the inner layer complexation of absorbents played a critical role in removing the herbicides [23]. The adsorptions of the herbicides for the GCRB and GCRB-N reached their equilibrium states within 12 h and 16 h, respectively. ALA, DIU, and SIM were not efficiently removed using the GCRB under the adsorption conditions (the removal rate of ALA = 6.0%, the removal rate of DIU = 4.7%, and the removal rate of SIM = 3.1%). Significant increases in the removal rates were found for the herbicides using the GCRB-N compared to the GCRB under the adsorption conditions (the removal rate of ALA = 56.6%, the removal rate of DIU = 80.6%, and the removal rate of SIM = 47.4%). These phenomena may indicate the differences in the physicochemical properties of the GCRB and GCRB-N.

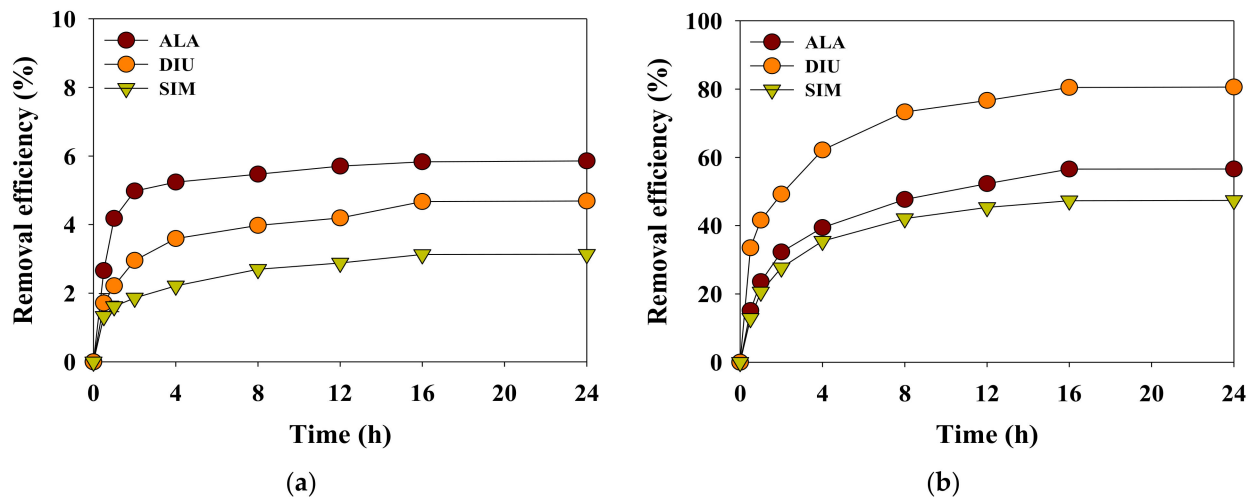


Figure 5. The adsorption kinetics of the herbicides on (a) the GCRB and (b) GCRB-N (agitation speed = 150 rpm, adsorbent dosage = 50 mg/L, initial concentration of each herbicide = 10 μ M, pH = 7.0, and temperature = 25 $^{\circ}$ C).

Table 3 presents the kinetic model parameters for the adsorption of the herbicides using the GCRB and GCRB-N. Based on the correlation coefficient values (R^2), the pseudo-second-order model ($R^2 = 0.995$ – 1.000) better explained the adsorption of the herbicides by the GCRB and GCRB-N than the pseudo first order model ($R^2 = 0.916$ – 0.993). The equilibrium adsorption capacities of the herbicides ($Q_{e,exp}$) on the GCRB-N were much bigger compared to those of the GCRB ($Q_{e,exp}$ of the GCRB = 6.53–11.74 μ mol g^{-1} , $Q_{e,exp}$ of the GCRB-N = 99.16–166.42 μ mol/g). The kinetics of the herbicide adsorptions on the GCRB and GCRB-N followed the pseudo-second-order model rather than the pseudo first order model. Besides, the $Q_{e,exp}$ values of ALA, DIU, and SIM toward the GCRB and GCRB-N were similar to their theoretical adsorption capacities ($Q_{e,cal}$) calculated using the pseudo second order equation (adsorption: $Q_{e,cal}$ of the GCRB = 6.85–12.00 μ mol/g, $Q_{e,cal}$ of the GCRB-N = 100.01–167.08 μ mol/g). These observations elucidate that the adsorption of the herbicides using the GCRB and GCRB-N is critically governed by chemical adsorption [28].

Table 3. Kinetic parameters for the adsorptions of herbicides using the GCRB and GCRB-N (agitation speed = 150 rpm, absorbent dosage = 50 mg/L, initial concentration of each herbicide = 10 μM , pH = 7.0, and temperature = 25 $^{\circ}\text{C}$).

Absorbents	Compounds	$Q_{e,exp}$ ($\mu\text{mol/g}$)	Pseudo-First-Order			Pseudo-Second-Order		
			$Q_{e,cal}$ ($\mu\text{mol/g}$)	k_1 (1/h)	R^2	$Q_{e,cal}$ ($\mu\text{mol/g}$)	k_2 ($\text{g}/\mu\text{mol}\cdot\text{h}$)	R^2
GCRB	ALA	11.74 ± 0.14	4.12 ± 0.25	0.17 ± 0.03	0.916	12.00 ± 0.08	0.13 ± 0.01	0.999
	DIU	9.95 ± 0.06	5.95 ± 0.56	0.14 ± 0.02	0.953	10.07 ± 0.001	0.06 ± 0.002	0.995
	SIM	6.53 ± 0.06	4.31 ± 0.70	0.19 ± 0.02	0.959	6.75 ± 0.05	0.10 ± 0.007	0.997
GCRB-N	ALA	122.71 ± 0.23	84.62 ± 2.04	0.14 ± 0.05	0.985	123.11 ± 0.07	0.004 ± 0.0003	0.996
	DIU	166.42 ± 0.66	97.69 ± 3.74	0.18 ± 0.006	0.989	167.08 ± 1.56	0.005 ± 0.0004	0.999
	SIM	99.16 ± 0.88	69.81 ± 3.71	0.21 ± 0.07	0.993	100.01 ± 1.88	0.006 ± 0.003	0.999

3.3. Adsorption Isotherms of Herbicides

The adsorption of the ALA, DIU, and SIM using the GCRB and GCRB-N were investigated with the Langmuir and Freundlich models (Table 4 and Figure 6). For the GCRB, the adsorptions of the herbicides were well matched to the Freundlich model with high R^2 values (Langmuir isotherm: $R^2 = 0.885$ – 0.919 ; Freundlich isotherm $R^2 = 0.999$). These results show that the herbicides responded to the heterogeneous GCRB surfaces [34]. The adsorptions of herbicides for the GCRB-N were better described by the Langmuir isotherm model ($R^2 = 0.999$) than the Freundlich isotherm model ($R^2 = 0.885$ – 0.982). This is evidence that the monolayer adsorption governed the removal of herbicides toward the homogeneous GCRB-N surfaces during the adsorption proceeding [35].

Table 4. Isotherm parameters for the competitive adsorptions of herbicides using the GCRB and GCRB-N (agitation speed = 150 rpm, contact period = 24 h, absorbent dosage = 50 mg/L, initial concentration of each herbicide = 10 μM , pH = 7.0, and temperature = 25 $^{\circ}\text{C}$).

Absorbents	Compounds	Langmuir			Freundlich		
		Q_{max} ($\mu\text{mol/g}$)	K_L ($\text{L}/\mu\text{mol}$)	R^2	n	K_F ($\mu\text{mol}^{1-(1/n)} \text{L}^{1/n}/\text{g}$)	R^2
GCRB	ALA	90.91 ± 1.72	0.006 ± 0.0003	0.919	1.15 ± 0.002	0.69 ± 0.007	0.999
	DIU	115.12 ± 1.38	0.004 ± 0.0004	0.885	1.10 ± 0.002	0.58 ± 0.0008	0.999
	SIM	106.38 ± 0.65	0.004 ± 0.0001	0.905	1.11 ± 0.001	0.54 ± 0.002	0.999
GCRB-N	ALA	231.48 ± 0.44	0.11 ± 0.0004	0.999	2.73 ± 0.004	51.05 ± 0.08	0.982
	DIU	322.58 ± 1.91	0.82 ± 0.05	0.999	5.13 ± 1.91	166.26 ± 0.05	0.885
	SIM	144.92 ± 0.55	0.15 ± 0.0009	0.999	3.72 ± 0.006	46.72 ± 0.03	0.980

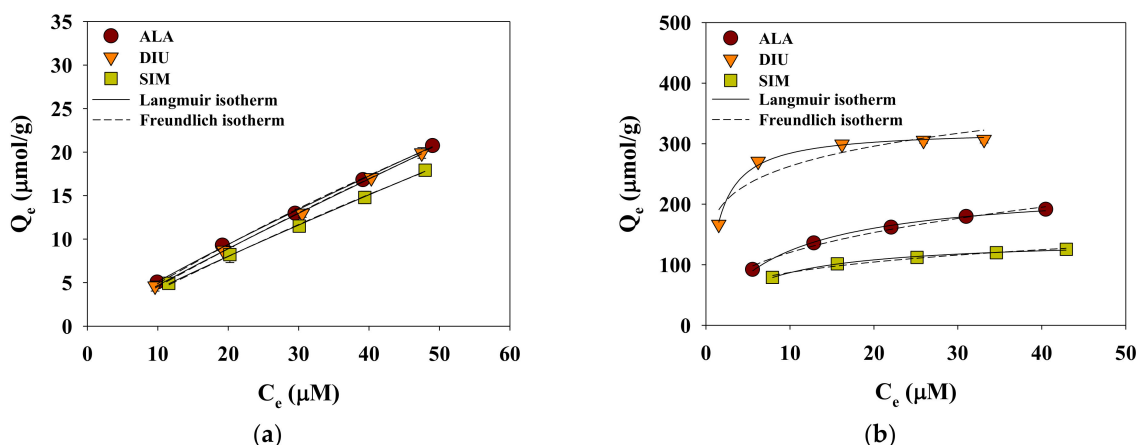


Figure 6. The adsorption isotherms of the herbicides on (a) the GCRB and (b) GCRB-N (agitation speed = 150 rpm, contact period = 24 h, absorbent dosage = 50 mg/L, initial concentration = 10–50 μM , pH = 7.0, and temperature = 25 $^{\circ}\text{C}$).

The adsorption affinities of herbicides to the GCRB and GCRB-N were estimated using the n values and the R_L values, respectively. The n values (dimensionless) of the Freundlich model using the GCRB were used to examine the adsorption affinity of the herbicides under the batch experiments: (i) $n > 1.0$ (favorable), (ii) $n = 1.0$ (linear), and (iii) $n < 1.0$ (unfavorable) [36]. The n values of ALA (1.15), DIU (1.10), and SIM (1.11) were favorable. The R_L values ($R_L = 1/(1 + K_L C_0)$), (i) $R_L = 0$: irreversible, (ii) $0 < R_L < 1$: favorable, (iii) $R_L = 1$: linear, and (iv) $R_L > 1$: unfavorable) of the Langmuir model were used to identify the maximum adsorption capacity of herbicides by GCRB-N [33]. The R_L values of GCRB-N were in the range of 0.109–0.470 (favorable). These observations supported that the change in the uniformity of the GCRB surface through the NaOH activation could improve the adsorption affinities of the herbicides (multilayer adsorption \rightarrow monolayer adsorption). Moreover, These results are comparable to the relative maximum adsorption capacity (K_F) calculated using different adsorbents, as shown in Table 5.

Table 5. Summary of available results related to herbicides adsorption by biochars.

Biomass	Pyrolysis Temperature (°C)	Application Matrix	Herbicides	Initial Concentration (μM)	1/n	K_F ($\mu\text{mol}^{1-(1/n)} \text{L}^{1/n}/\text{g}$)	References
Paper mill sludge	550	0.5%, Highly permeable red Ferrosol	DIU	4.3–43	0.67	133	[37]
Mixture of maple, elm, and oak woodchips and bark	450	Aqueous solution	SIM	0.248–24.8	0.68	2.55	[38]
Fly ash (Olive cake)	450	Aqueous solution	DIU	10.7	0.42	184	[39]
Ground coffee residues	800	Aqueous solution	ALA DIU SIM	10	0.37–0.87 0.19–0.91 0.27–0.90	0.69–51.05 0.58–166.26 0.54–46.72	This study

3.4. Effects of Solution pH on Adsorption of Herbicides

The differences in the removal efficiencies of the herbicides (i.e., ALA, DIU, and SIM) to identify the competitive adsorption of the pristine and alkali-activated GCR biochars as a function of the aqueous solution pH are depicted in Figure 7. The amount of adsorptions for ALA and SIM using the GCRB (pH 3: ALA = 14.12 $\mu\text{mol/g}$ and SIM = 6.40 $\mu\text{mol/g}$; pH 7: ALA = 12.23 $\mu\text{mol/g}$ and SIM = 6.35 $\mu\text{mol/g}$; pH 11: ALA = 7.77 $\mu\text{mol/g}$ and SIM = 4.72 $\mu\text{mol/g}$) and GCRB-N (pH 3: ALA = 129.62 $\mu\text{mol/g}$ and SIM = 108.25 $\mu\text{mol/g}$; pH 7: ALA = 122.77 $\mu\text{mol/g}$ and SIM = 100.61 $\mu\text{mol/g}$; pH 11: ALA = 115.99 $\mu\text{mol/g}$ and SIM = 89.38 $\mu\text{mol/g}$) were decreased in the pH range from 3 to 11. Moreover, the differences in the removal rates of herbicides by the GCRB and GCRB-N were in good agreement with the order of the Log D values of the ALA and SIM (pH 3: ALA (Log D = 3.59) > SIM (Log D = 0.60); pH 7: ALA (Log D = 3.59) > SIM (Log D = 1.78); pH 11: ALA (Log D = 3.59) > SIM (Log D = 1.78)). However, the adsorptions of DIU by the GCRB and GCRB-N were not influenced due to its high pK_a value (DIU = 13.18) under the different pH conditions. Furthermore, the amount of adsorptions for DIU using the GCRB (pH 3 = 7.78 $\mu\text{mol/g}$; pH 7 = 9.50 $\mu\text{mol/g}$; pH 11 = 10.62 $\mu\text{mol/g}$) and GCRB-N (pH 3 = 151.71 $\mu\text{mol/g}$; pH 7 = 158.54 $\mu\text{mol/g}$; pH 11 = 160.63 $\mu\text{mol/g}$) were increased. Fontecha-Ca'mara et al. (2007) have demonstrated that AC and DIU are predominated repulsive electrostatic interactions because the AC surface charge and DIU are positively charged at the acidic conditions [40]. In both neutral and alkaline conditions, AC and DIU are non-electrostatic interactions predominated, and the adsorption capacity is increased. These observations could be postulated that the differences in the hydrophobic and electrostatic interactions between herbicides and adsorbents at the different pH conditions governed the adsorptions of the herbicides using the GCRB and GCRB-N [23].

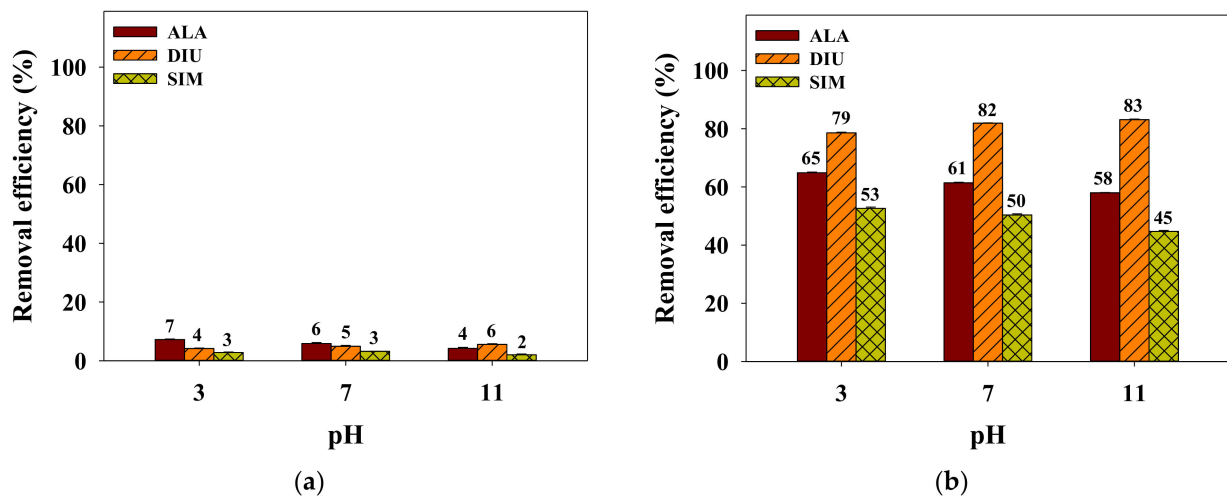


Figure 7. The effects of the solution pH on the removal of the herbicides by (a) GCRB and (b) GCRB-N (agitation speed = 150 rpm, contact period = 24 h, absorbent dosage = 50 mg/L, initial concentration of each herbicide = 10 μ M, and temperature = 25 $^{\circ}$ C).

3.5. Effects of Solution Temperature on Adsorption of Herbicides

The effects of temperature on the adsorption of herbicides using GCRB and GCRB-N are revealed in Figure 8. The removal efficiencies of herbicides using GCRB (15 $^{\circ}$ C: ALA = $2.9 \pm 0.1\%$, DIU = $2.2 \pm 0.1\%$, and SIM = $1.0 \pm 0.1\%$; 25 $^{\circ}$ C: ALA = $4.8 \pm 0.1\%$, DIU = $3.8 \pm 0.1\%$, and SIM = $2.0 \pm 0.1\%$; 35 $^{\circ}$ C: ALA = $6.6 \pm 0.1\%$, DIU = $5.8 \pm 0.4\%$, and SIM = $3.2 \pm 0.2\%$) and GCRB-N (15 $^{\circ}$ C: ALA = $57.1 \pm 0.3\%$, DIU = $73.2 \pm 0.1\%$, and SIM = $42.2 \pm 0.8\%$; 25 $^{\circ}$ C: ALA = $64.7 \pm 0.3\%$, DIU = $81.5 \pm 0.1\%$, and SIM = $52.3 \pm 0.1\%$; 35 $^{\circ}$ C: ALA = $73.7 \pm 0.4\%$, DIU = $84.9 \pm 0.1\%$, and SIM = $62.2 \pm 0.6\%$) were progressively increased with increasing the temperature. However, the adsorption trends for the herbicides by the GCRB and GCRB-N were significantly different (the GCRB: ALA > DIU > SIM; the GCRB-N: DIU > ALA > SIM) at the different temperature conditions. Similar behaviors were observed to remove the micropollutants by absorbents under different temperature conditions [41,42].

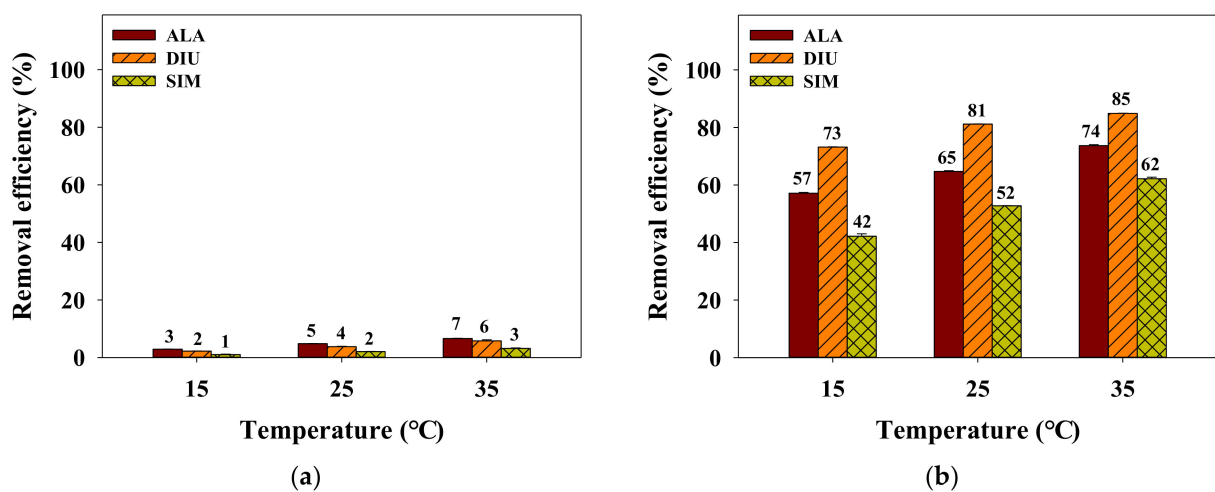


Figure 8. The effects of the solution temperature on the removal of the herbicides by (a) the GCRB and (b) GCRB-N (agitation speed = 150 rpm, contact period = 24 h, absorbent dosage = 50 mg/L, initial concentration of each herbicide = 10 μ M, and pH 7).

3.6. Effects of Ionic Strength on Adsorption of Herbicides

The effects of ionic strength on the adsorption of the herbicides by GCRB and GCRB-N were illustrated in Figure 9. The removal rates of herbicides using the GCRB and GCRB-N were gradually increased with increasing ionic strengths (the GCRB: the removal rate of ALA = 3.6% → 6.9%, the removal rate of DIU = 2.0% → 6.3%, the removal rate of SIM = 1.5% → 6.1%; the GCRB-N: the removal rate of ALA = 61.4% → 70.2%, the removal rate of DIU = 81.4% → 87.5%, the removal rate of SIM = 47.0% → 60.3%). These observations could describe that the decreased solubility of the organic compounds with high concentrations of sodium ions might promote the adsorption capacity of the porous carbonaceous adsorbents under different ionic strength conditions (salting-out effects) [43,44].

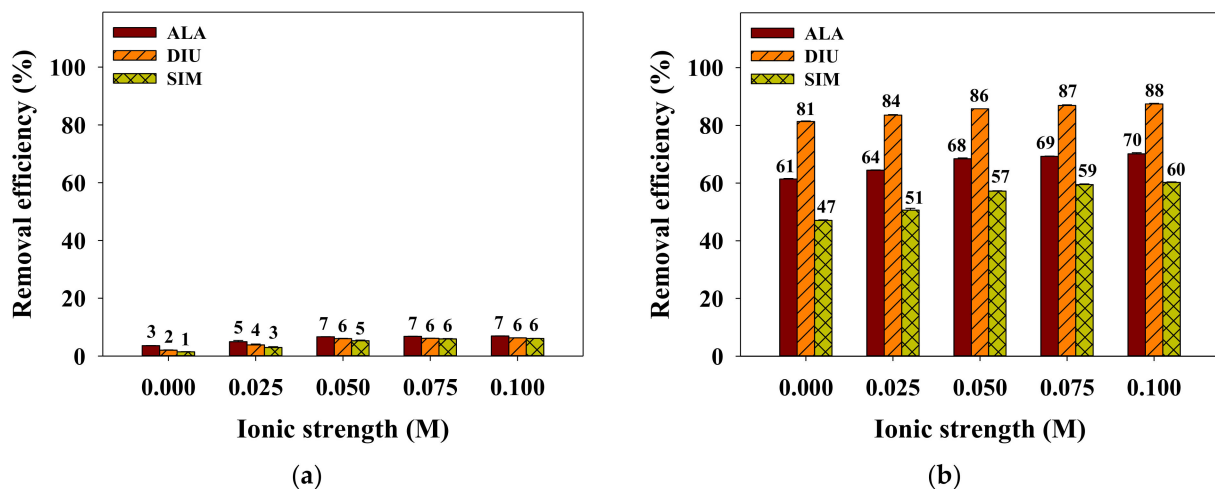


Figure 9. The effects of ionic strength on the removal of the herbicides by (a) the GCRB and (b) GCRB-N (agitation speed = 150 rpm, contact period = 24 h, adsorbent dosage = 50 mg/L, initial concentration of each herbicide = 10 μ M, pH 7, and temperature = 25 $^{\circ}$ C).

3.7. Effects of Humic Acids on Adsorption of Herbicides

The interferences of humic acids on the adsorptions of the herbicides for the GCRB and GCRB-N are compared in Figure 10. The removal rates of herbicides using the GCRB was slightly reduced in the presence of the humic acids (the removal rate without humic acids: ALA = 6.0 \pm 0.1%, DIU = 5.0 \pm 0.1%, and SIM = 3.2 \pm 0.1%; the removal rate with humic acids: ALA = 5.5 \pm 0.1%, DIU = 4.5 \pm 0.2%, and SIM = 2.9 \pm 0.3%). The removal rates of ALA and SIM using the GCRB-N were considerably reduced due to the competition with humic acids (the removal rate without humic acids: ALA = 61.4 \pm 0.2% and SIM = 49.5 \pm 0.4%; the removal rate with humic acids: ALA = 57.3 \pm 0.2% and SIM = 43.9 \pm 0.5%) [35]. However, the removal rates of DIU by the GCRB-N were not significantly affected by the presence of humic acids (the removal rate without humic acids: DIU = 81.9 \pm 0.1%; the removal rate with humic acids: DIU = 81.9 \pm 0.2%). This result could be explained that DIU was not significantly affected by the humic acids for the GCRB-N. Similar behavior was observed for the outcompeting of the micropollutant adsorption by the biochars at the neutral pH condition in the humic acid presence [23].

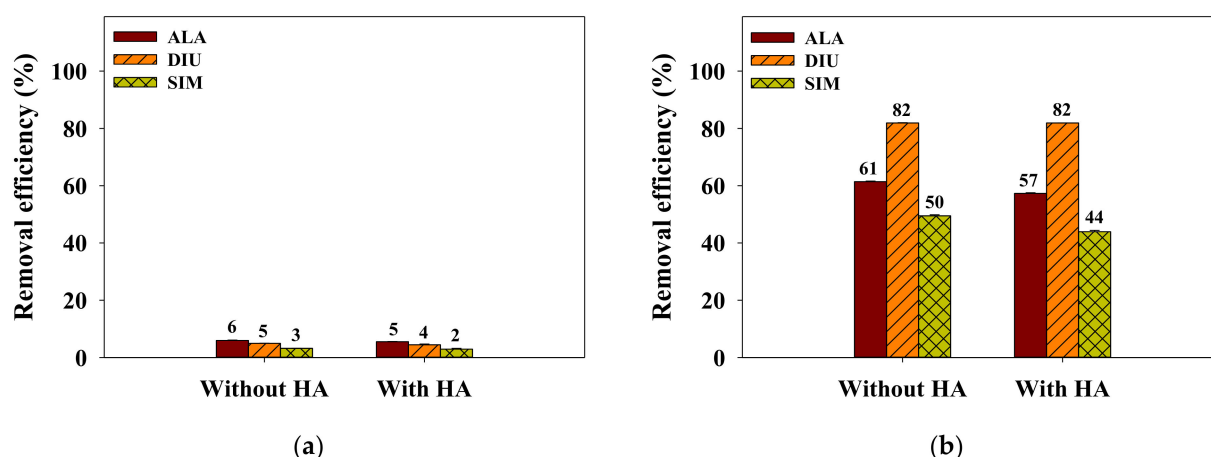


Figure 10. The effects of humic acids on the removal of the herbicides by (a) the GCRB and (b) GCRB-N (concentration of humic acids = 5 mg/L, agitation speed = 150 rpm, contact period = 24 h, adsorbent dosage = 50 mg/L, initial concentration of each herbicide = 10 μ M, pH 7, and temperature = 25 $^{\circ}$ C).

4. Conclusions

This study investigated the effects of the NaOH activation on the physicochemical characteristics of GCRB related to the adsorptions of the herbicides (ALA, DIU, and SIM). The specific surface area and pore volume of GCRB-N presented approximately 106 times and 21 times greater than those of the GCRB. These results were intimately connected to the adsorption capacities of the GCRB and GCRB-N ($Q_{e,exp}$ of the GCRB-N = 99.16–122.71 μ mol/g and the GCRB = 6.53–11.74 μ mol/g). The pseudo second order kinetics ($R^2 = 0.995$ – 0.999) were well matched to the adsorptions of the herbicides using the GCRB and GCRB-N than the pseudo first order kinetics ($R^2 = 0.916$ – 0.993), indicating that the chemisorption predominantly governed the adsorptions. The adsorption of the herbicides by the GCRB followed the Freundlich model (R^2 of Langmuir model = 0.885–0.919, R^2 of Freundlich model = 0.999), whereas the Langmuir model was fitted to the adsorption of the GCRB-N (R^2 of Langmuir model = 0.999, R^2 of Freundlich model = 0.885–0.982). The order of the removal rates of the herbicides by the GCRB and GCRB-N at the different pH values was significantly affected by the differences in the hydrophobic and electrostatic interactions between herbicides and adsorbents. The removal rates of herbicides using GCRB and GCRB-N were gradually enlarged with increasing temperature. Moreover, the salting-out effects prominent in the existence of high concentrations of sodium ions could enhance the adsorptions of the herbicides for the GCRB and GCRB-N. Although the humic acids might inhibit the adsorption of the herbicides by the GCRB and GCRB-N, the removal rates of the herbicides by the GCRB-N (43.9–81.9%) were higher than those of the GCRB (2.9–5.5%). These findings might conclude that the NaOH activation might be a promising method to enhance the adsorption capacities of GCRB practically applicable for removing herbicides from the water and wastewater treatment process.

Author Contributions: Conceptualization, Y.-G.L.; methodology, Y.-G.L.; validation, Y.-G.L.; formal analysis, J.S. and J.K.; investigation, S.K. and C.S.; data curation, Y.-G.L.; writing—original draft preparation, Y.-G.L.; writing—review and editing, K.H.C. and K.C.; supervision, K.C.; funding acquisition, K.H.C. All authors have read and agreed to the published version of the manuscript.

Funding: This work was supported by the National Research Foundation of Korea (NRF) grant funded by the Korea government (MSIT) (No. 2020R1A4A1019568).

Conflicts of Interest: The authors declare no conflict of interest.

Abbreviations

ALA	Alachlor
C_e	Concentration of herbicides at equilibrium ($\mu\text{mol/L}$)
C_0	Initial concentrations of herbicides ($\mu\text{mol/L}$)
DIU	Diuron
GCRB	Ground coffee residue biochar
GCRB-N	NaOH activated ground coffee residue biochar
k_1	Pseudo-first-order rate constant (1/h)
k_2	Pseudo-second-order rate constant ($\text{g}/\mu\text{mol}\cdot\text{h}$)
K_F	Freundlich isotherm capacity factor ($\mu\text{mol}^{1-(1/n)} \text{L}^{1/n}/\text{g}$)
K_L	The adsorption energy ($\text{L}/\mu\text{mol}$)
Q_e	The quantities of the adsorbed herbicides at equilibrium ($\mu\text{mol/g}$)
Q_t	The amounts of the adsorbed herbicides at time t ($\mu\text{mol/g}$)
$Q_{e,\text{exp}}$	The adsorption capacities of the herbicides at equilibrium ($\mu\text{mol/g}$)
Q_{max}	The maximum adsorption capacity ($\mu\text{mol/g}$)
n	The adsorption affinity of the herbicides
SIM	Simazine
V	Volume of herbicides solution (L)

References

- Taha, S.M.; Amer, M.E.; Elmarsafy, A.E.; Elkady, M.Y. Adsorption of 15 different pesticides on untreated and phosphoric acid treated biochar and charcoal from water. *J. Environ. Chem. Eng.* **2014**, *2*, 2013–2025. [[CrossRef](#)]
- Tirmenstein, M.A.; Mangipudy, R. Alachlor. In *Encyclopedia of Toxicology*, 3rd ed.; Wexler, P., Ed.; Academic Press: Oxford, UK, 2014; pp. 107–109. [[CrossRef](#)]
- Antoniou, M.G.; De La Cruz, A.A.; Pelaez, M.A.; Han, C.; He, X.; Dionysiou, D.D.; Song, W.; O’Shea, K.E.; Ho, L.; Newcombe, G. Practices that prevent the formation of cyanobacterial blooms in water resources and remove cyanotoxins during physical treatment of drinking water. *Sci. Inventory* **2013**, *2*, 173–195.
- Vanraes, P.; Wardenier, N.; Surmont, P.; Lynen, F.; Nikiforov, A.; Van Hulle, S.W.H.; Leys, C.; Bogaerts, A. Removal of alachlor, diuron and isoproturon in water in a falling film dielectric barrier discharge (DBD) reactor combined with adsorption on activated carbon textile: Reaction mechanisms and oxidation by-products. *J. Hazard. Mater.* **2018**, *354*, 180–190. [[CrossRef](#)]
- Rosenfeld, P.E.; Feng, L. *Risks of Hazardous Wastes*, 1st ed.; William Andrew: Oxford, UK, 2011.
- Swan, S.; Guillette, L., Jr.; Myers, J.; vom Saal, F. Epidemiological studies of reproductive effects in humans. *Reprod. Toxicol.* **2008**, *19*, 5–26. [[CrossRef](#)]
- Magnusson, M.; Heimann, K.; Quayle, P.; Negri, A.P. Additive toxicity of herbicide mixtures and comparative sensitivity of tropical benthic microalgae. *Mar. Pollut. Bull.* **2010**, *60*, 1978–1987. [[CrossRef](#)] [[PubMed](#)]
- Zimba, P.V.; Tucker, C.S.; Mischke, C.C.; Grimm, C.C. Short-term effect of diuron on catfish pond ecology. *North Am. J. Aquac.* **2002**, *64*, 16–23. [[CrossRef](#)]
- Li, L.; Zhang, Y.; Zheng, L.; Lu, S.; Yan, Z.; Ling, J. Occurrence, distribution and ecological risk assessment of the herbicide simazine: A case study. *Chemosphere* **2018**, *204*, 442–449. [[CrossRef](#)]
- Sai, L.; Liu, Y.; Qu, B.; Yu, G.; Guo, Q.; Bo, C.; Xie, L.; Jia, Q.; Li, Y.; Li, X. The effects of simazine, a chlorotriazine herbicide, on the expression of genes in developing male *Xenopus laevis*. *Bull. Environ. Contam. Toxicol.* **2015**, *95*, 157–163. [[CrossRef](#)] [[PubMed](#)]
- Oropesa, A.; García Cambero, J.; Soler, F. Effect of long-term exposure to simazine on brain and muscle acetylcholinesterase activity of common carp (*Cyprinus carpio*). *Environ. Toxicol. Int. J.* **2008**, *23*, 285–293. [[CrossRef](#)] [[PubMed](#)]
- Leovac, A.; Vasyukova, E.; Ivančev-Tumbas, I.; Uhl, W.; Kragulj, M.; Tričković, J.; Kerkez, Đ.; Dalmacija, B. Sorption of atrazine, alachlor and trifluralin from water onto different geosorbents. *RSC Adv.* **2015**, *5*, 8122–8133. [[CrossRef](#)]
- Hnatukova, P.; Kopecka, I.; Pivokonsky, M. Adsorption of cellular peptides of *Microcystis aeruginosa* and two herbicides onto activated carbon: Effect of surface charge and interactions. *Water Res.* **2011**, *45*, 3359–3368. [[CrossRef](#)]
- Foo, K.; Hameed, B. Detoxification of pesticide waste via activated carbon adsorption process. *J. Hazard. Mater.* **2010**, *175*, 1–11. [[CrossRef](#)] [[PubMed](#)]
- Chingombe, P.; Saha, B.; Wakeman, R. Surface modification and characterisation of a coal-based activated carbon. *Carbon* **2005**, *43*, 3132–3143. [[CrossRef](#)]
- Lehmann, J.; Joseph, S. Biochar for environmental management: An introduction. *Biochar Environ. Manag. Sci. Technol.* **2009**, *1*, 1–12.
- Suo, F.; You, X.; Ma, Y.; Li, Y. Rapid removal of triazine pesticides by P doped biochar and the adsorption mechanism. *Chemosphere* **2019**, *235*, 918–925. [[CrossRef](#)] [[PubMed](#)]
- Suo, F.; Liu, X.; Li, C.; Yuan, M.; Zhang, B.; Wang, J.; Ma, Y.; Lai, Z.; Ji, M. Mesoporous activated carbon from starch for superior rapid pesticides removal. *Int. J. Biol. Macromol.* **2019**, *121*, 806–813. [[CrossRef](#)] [[PubMed](#)]

19. Zhou, Y.; Liu, X.; Xiang, Y.; Wang, P.; Zhang, J.; Zhang, F.; Wei, J.; Luo, L.; Lei, M.; Tang, L. Modification of biochar derived from sawdust and its application in removal of tetracycline and copper from aqueous solution: Adsorption mechanism and modelling. *Bioresour. Technol.* **2017**, *245*, 266–273. [[CrossRef](#)]
20. Fan, Q.; Sun, J.; Chu, L.; Cui, L.; Quan, G.; Yan, J.; Hussain, Q.; Iqbal, M. Effects of chemical oxidation on surface oxygen-containing functional groups and adsorption behavior of biochar. *Chemosphere* **2018**, *207*, 33–40. [[CrossRef](#)]
21. Choi, I.S.; Ko, S.H.; Kim, H.M.; Yang, J.E.; Jeong, S.-G.; Chang, J.Y.; Lee, K.H.; Qi, S.-B.; Xin, Q.; Cui, C.-B.; et al. Coffee residue as a valorization bio-agent for shelf-life extension of lactic acid bacteria under cryopreservation. *Waste Manag.* **2020**, *118*, 585–590. [[CrossRef](#)]
22. Karmee, S.K. A spent coffee grounds based biorefinery for the production of biofuels, biopolymers, antioxidants and biocomposites. *Waste Manag.* **2018**, *72*, 240–254. [[CrossRef](#)]
23. Shin, J.; Lee, Y.-G.; Lee, S.-H.; Kim, S.; Ochir, D.; Park, Y.; Kim, J.; Chon, K. Single and competitive adsorptions of micropollutants using pristine and alkali-modified biochars from spent coffee grounds. *J. Hazard. Mater.* **2020**, *400*, 123102. [[CrossRef](#)] [[PubMed](#)]
24. Víglašová, E.; Galamboš, M.; Danková, Z.; Krivosudský, L.; Lengauer, C.L.; Hood-Nowotny, R.; Soja, G.; Rompel, A.; Matík, M.; Briančin, J. Production, characterization and adsorption studies of bamboo-based biochar/montmorillonite composite for nitrate removal. *Waste Manag.* **2018**, *79*, 385–394. [[CrossRef](#)] [[PubMed](#)]
25. Yuan, H.; Lu, T.; Zhao, D.; Huang, H.; Noriyuki, K.; Chen, Y. Influence of temperature on product distribution and biochar properties by municipal sludge pyrolysis. *J. Mater. Cycles Waste Manag.* **2013**, *15*, 357–361. [[CrossRef](#)]
26. Ahmed, M.B.; Zhou, J.L.; Ngo, H.H.; Guo, W.; Johir, M.A.H.; Sornalingam, K. Single and competitive sorption properties and mechanism of functionalized biochar for removing sulfonamide antibiotics from water. *Chem. Eng. J.* **2017**, *311*, 348–358. [[CrossRef](#)]
27. Xiao, B.; Dai, Q.; Yu, X.; Yu, P.; Zhai, S.; Liu, R.; Guo, X.; Liu, J.; Chen, H. Effects of sludge thermal-alkaline pretreatment on cationic red X-GRL adsorption onto pyrolysis biochar of sewage sludge. *J. Hazard. Mater.* **2018**, *343*, 347–355. [[CrossRef](#)] [[PubMed](#)]
28. Li, M.; Zhao, Z.; Wu, X.; Zhou, W.; Zhu, L. Impact of mineral components in cow manure biochars on the adsorption and competitive adsorption of oxytetracycline and carbaryl. *RSC Adv.* **2017**, *7*, 2127–2136. [[CrossRef](#)]
29. Jin, H.; Capareda, S.; Chang, Z.; Gao, J.; Xu, Y.; Zhang, J. Biochar pyrolytically produced from municipal solid wastes for aqueous As(V) removal: Adsorption property and its improvement with KOH activation. *Bioresour. Technol.* **2014**, *169*, 622–629. [[CrossRef](#)]
30. Cho, D.-W.; Yoon, K.; Kwon, E.E.; Biswas, J.K.; Song, H. Fabrication of magnetic biochar as a treatment medium for As(V) via pyrolysis of FeCl₃-pretreated spent coffee ground. *Environ. Pollut.* **2017**, *229*, 942–949. [[CrossRef](#)] [[PubMed](#)]
31. Kim, H.-B.; Kim, S.-H.; Jeon, E.-K.; Kim, D.-H.; Tsang, D.C.W.; Alessi, D.S.; Kwon, E.E.; Baek, K. Effect of dissolved organic carbon from sludge, Rice straw and spent coffee ground biochar on the mobility of arsenic in soil. *Sci. Total Environ.* **2018**, *636*, 1241–1248. [[CrossRef](#)] [[PubMed](#)]
32. Baharum, N.A.; Nasir, H.M.; Ishak, M.Y.; Isa, N.M.; Hassan, M.A.; Aris, A.Z. Highly efficient removal of diazinon pesticide from aqueous solutions by using coconut shell-modified biochar. *Arab. J. Chem.* **2020**, *13*, 6106–6121. [[CrossRef](#)]
33. Shin, J.; Lee, Y.-G.; Kwak, J.; Kim, S.; Lee, S.-H.; Park, Y.; Lee, S.-D.; Chon, K. Adsorption of radioactive strontium by pristine and magnetic biochars derived from spent coffee grounds. *J. Environ. Chem. Eng.* **2021**, *9*, 105119. [[CrossRef](#)]
34. Lee, K.-H.; Lee, Y.-G.; Shin, J.; Chon, K.; Lee, S.-H. Selective Immobilization of Antimony Using Brucite-rich Precipitate Produced during In Situ Hypochlorous Acid Formation through Seawater Electrolysis in a Nuclear Power Plant. *Energies* **2020**, *13*, 4493. [[CrossRef](#)]
35. Kim, E.; Jung, C.; Han, J.; Her, N.; Park, C.M.; Jang, M.; Son, A.; Yoon, Y. Sorptive removal of selected emerging contaminants using biochar in aqueous solution. *J. Ind. Eng. Chem.* **2016**, *36*, 364–371. [[CrossRef](#)]
36. Kim, H.; Ko, R.-A.; Lee, S.; Chon, K. Removal Efficiencies of Manganese and Iron Using Pristine and Phosphoric Acid Pre-Treated Biochars Made from Banana Peels. *Water* **2020**, *12*, 1173. [[CrossRef](#)]
37. Martin, S.M.; Kookana, R.S.; Van Zwieten, L.; Krull, E. Marked changes in herbicide sorption–desorption upon ageing of biochars in soil. *J. Hazard. Mater.* **2012**, *231–232*, 70–78. [[CrossRef](#)]
38. Zheng, W.; Guo, M.; Chow, T.; Bennett, D.N.; Rajagopalan, N. Sorption properties of greenwaste biochar for two triazine pesticides. *J. Hazard. Mater.* **2010**, *181*, 121–126. [[CrossRef](#)]
39. Quirantes, M.; Nogales, R.; Romero, E. Sorption potential of different biomass fly ashes for the removal of diuron and 3,4-dichloroaniline from water. *J. Hazard. Mater.* **2017**, *331*, 300–308. [[CrossRef](#)] [[PubMed](#)]
40. Fontecha-Cámara, M.; López-Ramón, M.; Alvarez-Merino, M.; Moreno-Castilla, C. Effect of surface chemistry, solution pH, and ionic strength on the removal of herbicides diuron and amitrole from water by an activated carbon fiber. *Langmuir* **2007**, *23*, 1242–1247. [[CrossRef](#)] [[PubMed](#)]
41. Tong, Y.; Mayer, B.K.; McNamara, P.J. Adsorption of organic micropollutants to biosolids-derived biochar: Estimation of thermodynamic parameters. *Environ. Sci. Water Res. Technol.* **2019**, *5*, 1132–1144. [[CrossRef](#)]
42. Chen, C.; Chen, D.; Xie, S.; Quan, H.; Luo, X.; Guo, L. Adsorption behaviors of organic micropollutants on zirconium metal–organic framework UiO-66: Analysis of surface interactions. *ACS Appl. Mater. Interfaces* **2017**, *9*, 41043–41054. [[CrossRef](#)]
43. Xiao, X.; Sheng, G.D.; Qiu, Y. Improved understanding of tributyltin sorption on natural and biochar-amended sediments. *Environ. Toxicol. Chem.* **2011**, *30*, 2682–2687. [[CrossRef](#)] [[PubMed](#)]
44. Xiang, Y.; Xu, Z.; Zhou, Y.; Wei, Y.; Long, X.; He, Y.; Zhi, D.; Yang, J.; Luo, L. A sustainable ferromanganese biochar adsorbent for effective levofloxacin removal from aqueous medium. *Chemosphere* **2019**, *237*, 124464. [[CrossRef](#)] [[PubMed](#)]